considerable destabilization of the $10b_1$ MO (dominantly phosphorus 3p) by the nitrogen lone pairs. One really has an NPN three-center, four-electron "π system" familiar from the allyl radical anion and other systems showing an NPN moiety.[11] The nitrogen lone pair electrons occupy the bonding $9b_1$ MO (and the formally nonbonding a_2 MO), and only the antibonding "π MO" ($10b_1$) of the three-center system is available on the P side for the open-shell state. This view is confirmed by the near planarity of N in the molecules investigated. The out-of-plane angle is 9° for the parent molecule **1** with R = R′ = H (at the C_2 equilibrium geometry) and only 0.2° for R = *i*-Pr and R′ = Me (the out-of-plane angle in ammonia is 61.4°). As further support we point out that the shortest PN distance (159.3 pm) of the cases considered in Table II occurs for the 90° twisted $^1A_1$ state, where the "allylic" system is unperturbed by the PC "double bond", whereas the longest PN bond occurs in the $^3A_2$ state where the singly occupied $10b_1$ MO is PN antibonding.

In Table II we have also given the PC "shared electron numbers" (SEN) of the population analysis,[12] which are a measure for covalent bond strength. We recall for comparison that SEN $\approx$ 1.4 and SEN $\approx$ 2.2 correspond to strong covalent single and double bonds. In the (almost) planar structures *and* the 90° $^1A_1$ structure of $(NH_2)_2P^+{=}C(SiH_3)_2$, we find SEN $\approx$ 2. The remaining cases yield SEN $\leq$ 1.4. The SEN(PC) are thus in line with the computed structure constants and the interpretations given above.

The comparison between **1** with R = R′ = H and **2** with R = R′ = Me confirms the conclusion drawn on the basis of net atomic charges presented in Table I: the amino and silyl groups in **1** are of great importance since they lead to a certain degree of Y conjugation resulting in properties which differ markedly from those expected for phosphanylcarbenes **2**.

The computed twist angle for **1** with R = *i*-Pr, R′ = Me is 40°, in relatively poor agreement with the experimental value of 60°. There are various possible sources for this discrepancy. We have assumed C_2 symmetry (leading already to 102 internal degrees of freedom), whereas a slight distortion to C_1 is found in the crystal. More important is the relatively small rotational barrier of the PC double bond in **1**, discussed above, which makes the twist angle sensitive to approximations inherent in the present approach (small basis sets for Me and *i*-Pr which underestimate steric requirements, neglect of electron correlation), and possibly also to crystal-packing effects. The remaining computed structure parameters deviate only by a few picometers or degrees from experiment[1] (in parentheses) for **1** with R = *i*-Pr, R′ = Me (in picometers and degrees, atoms labeled as in Figure 1a if confusion is possible): PC = 161.6 (162.0), PN = 162.8 (161.5/161.0), SiC2 = 195.0 (187.5/191.3), ∠NPN = 114.3 (112.2), ∠C2PN = 122.8 (123.4/124.4), ∠PNC7 = 122.6 (121.0/124.4), ∠PNC9 = 124.9 (120.2/123.1) ∠C7NC9 = 112.4 (115.1/115.6), ∠PC2Si = 121.6 (119.3/121.7), ∠SiC2Si = 116.8 (119.1); sum of bond angles at N is 359.9 (359.7).

(11) Schiffer, H.; Ahlrichs, R.; Häser, M. *Theor. Chim. Acta* **1989**, *75*, 1.

(12) Ehrhardt, C.; Ahlrichs, R. *Theor. Chim. Acta* **1985**, *68*, 231.

III. Summary

The combination of a short PC bond distance and a large twist angle in **1** may be rationalized in the following way. The Coulomb bond stabilization acts independently of the twist angle. The slight polarity of the PC bond in phosphanylcarbenes **2** becomes much more pronounced in **1**, which has some degree of Y conjugation and is further enhanced by silyl groups. This together with some degree of PC $2p\pi 3d\pi$ bonding in the 90° twisted structure leads to a rotational barrier around the PC bond of only 20 kcal/mol, in **1** with R = R′ = H, which facilitates twisting due to steric requirements of bulky groups R and R′ in **1**.

The remarkable structural features of **1**, R = *i*-Pr and R′ = Me, found by Bertrand et al.,[1] are thus essentially due to pronounced changes in molecular electronic structure effected by the electronegative NR_2 groups at P and the electropositive SiR_3 groups at C, which facilitate twisting caused by steric hindrance of bulky groups R and R′ in **1**. The present discussion of structural features of **1** is based on trends in computed properties (structure, atomic charges) resulting from changes in substituents. This view is complementary to—certainly not in contradiction with—the model of Trinquier and Malrieu[13] based on properties of the radicals obtained by breaking the double bond.

Acknowledgment. The authors thank Dr. G. Bertrand for valuable discussions. This work has been supported by the Fonds der Chemischen Industrie.

Supplementary Material Available: Listing of Cartesian coordinates of atoms, basis sets, and SCF energies of all molecules treated in this paper (11 pages). Ordering information is given on any current masthead page.

(13) Trinquier, G.; Malrieu, J. P. *J. Am. Chem. Soc.* **1987**, *109*, 5303.

MNDO Study of Large Carbon Clusters

Dirk Bakowies and Walter Thiel*

Contribution from Theoretische Chemie, Universität GH Wuppertal, 5600 Wuppertal 1, Germany.
Received October 22, 1990

Abstract: MNDO calculations with complete geometry optimization are reported for 30 polyhedral carbon clusters C_n ($20 \leq n \leq 540$). The MNDO results for a planar graphite sheet are extrapolated from calculations on D_{6h} hydrocarbons C_nH_m ($n = 6k^2$, $m = 6k$, $k = 1$–6) and used as a reference for discussing the properties of the clusters. The structural features of the clusters are correlated with their stability. The relative MNDO energies with respect to graphite are compared with curvature-corrected Hückel calculations and with force field estimates, and criteria for the stability of the clusters are discussed. Infrared spectra are predicted for six stable clusters. Several cationic lithium complexes and their interconversions are investigated for C_{60} and C_{42}. Finally, computational aspects and performance data are considered, particularly for the largest clusters studied.

1. Introduction

Over the past years there has been considerable interest in pure carbon molecules. A comprehensive review[1] has recently documented the structural, electronic, and spectroscopic properties of small C_n molecules ($n < 20$) whose most stable isomers are usually either linear chains or monocyclic rings. Larger carbon clusters with $n \leq 190$ have been generated[2] by laser vaporization of graphite into a supersonic beam, followed by photoionization and

(1) Weltner, W., Jr.; van Zee, R. J. *Chem. Rev.* **1989**, *89*, 1713.

(2) Rohlfing, E. A.; Cox, D. M.; Kaldor, A. *J. Chem. Phys.* **1984**, *81*, 3322.

0002-7863/91/1513-3704$02.50/0

mass spectrometric detection. Only clusters with an even number of atoms were observed for $n \geq 40$. Under certain experimental conditions[3] the mass spectrum is dominated by the C_{60} peak which has been assigned to a "superstable" cluster with a truncated icosahedral structure (buckminsterfullerene).[3] Subsequently, all observed even-numbered carbon clusters with $n \geq 32$ have been suggested to correspond to polyhedral, spheroidal cage structures.[4,5] After considerable experimental activity, there is now an extensive literature concerning e.g. the formation processes and relative abundancies of different clusters[6-13] (up to $n \approx 600$[13]), their laser-induced fragmentation processes,[5,14] their metastable decay,[15] their reactivity toward small molecules,[4] and the properties of their metal complexes.[12,16-18] However, accurate experimental data on the structures of large carbon clusters are still lacking, and there are only a few spectroscopic data available, mainly for C_{60} (UV,[19] UPS,[20] IR[21]).

Polyhedral carbon clusters have been suggested to play an important role in the formation and morphology of soot[4], and a detailed carbon nucleation scheme has been developed[22-24] which leads to concentric spiral-shell species with overall quasi-icosahedral shape. The relevance of polyhedral clusters to soot formation has been debated,[25] but it is supported by high-resolution electron micrographs of partially graphitized carbon[26] and by the observation of even-numbered polyhedral carbon ions ($30 \leq n \leq 210$) in sooting hydrocarbon flames.[27] It has also been proposed[22,23,28] that C_{60} may be promiment in the circumstellar dust of carbon-rich stars and in interstellar matter although an initial search for interstellar bands of C_{60} has not been successful.[29]

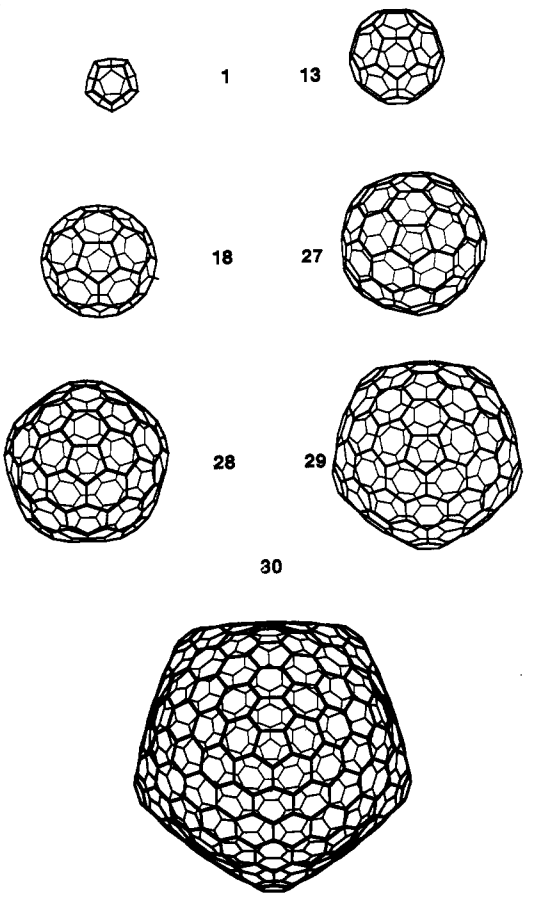

Figure 1. Clusters of type A with topological I_h or I symmetry. The numbering refers to Tables III and IV.

On the theoretical side, most of the work has concentrated on buckminsterfullerene C_{60}. Following early speculations on the existence of carbon cages,[30] calculations based on Hückel theory, resonance theory, or related methods[31-49] have found buckminsterfullerene to be an aromatic closed-shell molecule with a π resonance stabilization whose magnitude depends on the choice of reference.[35,45,47,50] Some of these calculations take into account that the π interaction is diminished by the curvature of the cluster.[42,43,47] The geometry of C_{60} has been optimized at the MNDO,[51,52] AM1,[53,54] INDO,[55] PRDDO,[56] and ab initio SCF

(3) Kroto, H. W.; Heath, J. R.; O'Brien, S. C.; Curl, R. F.; Smalley, R. E. *Nature* **1985**, *318*, 162.
(4) Zhang, Q. L.; O'Brien, S. C.; Heath, J. R.; Liu, Y.; Curl, R. F.; Kroto, H. W.; Smalley, R. E. *J. Phys. Chem.* **1986**, *90*, 525.
(5) O'Brien, S. C.; Heath, J. R.; Curl, R. F.; Smalley, R. E. *J. Chem. Phys.* **1988**, *88*, 220.
(6) Bloomfield, L. A.; Geusic, M. E.; Freeman, R. R.; Brown, W. L. *Chem. Phys. Lett.* **1985**, *121*, 33.
(7) Liu, Y.; O'Brien, S. C.; Zhang, Q. L.; Heath, J. R.; Tittel, F. K.; Curl, R. F.; Kroto, H. W.; Smalley, R. E. *Chem. Phys. Lett.* **1986**, *126*, 215.
(8) Cox, D. M.; Trevor, D. J.; Reichmann, K. C.; Kaldor, A. *J. Am. Chem. Soc.* **1986**, *108*, 2457.
(9) Hahn, M. Y.; Honea, E. C.; Paguia, A. J.; Schriver, K. E.; Camarena, A. M.; Whetten, R. L. *Chem. Phys. Lett.* **1986**, *130*, 12.
(10) O'Keefe, A.; Ross, M. M.; Baronavski, A. P. *Chem. Phys. Lett.* **1986**, *130*, 17.
(11) O'Brien, S. C.; Heath, J. R.; Kroto, H. W.; Curl, R. F.; Smalley, R. E. *Chem. Phys. Lett.* **1986**, *132*, 99.
(12) Cox, D. M.; Reichmann, K. C.; Kaldor, A. *J. Chem. Phys.* **1988**, *88*, 1588.
(13) So, H. Y.; Wilkins, C. L. *J. Phys. Chem.* **1989**, *93*, 1184.
(14) Geusic, M. E.; Jarrold, M. F.; McIlrath, T. J.; Freeman, R. R.; Brown, W. L. *J. Chem. Phys.* **1987**, *86*, 3862.
(15) Radi, P. P.; Brunn, T. L.; Kemper, P. R.; Molchan, M. E.; Bowers, M. T. *J. Chem. Phys.* **1988**, *88*, 2809.
(16) Heath, J. R.; O'Brien, S. C.; Zhang, Q.; Liu, Y.; Curl, R. F.; Kroto, H. W.; Tittel, F. K.; Smalley, R. E. *J. Am. Chem. Soc.* **1985**, *107*, 7779.
(17) Cox, D. M.; Trevor, D. J.; Reichmann, K. C.; Kaldor, A. *J. Am. Chem. Soc.* **1986**, *108*, 2457.
(18) Weiss, F. D.; Elkind, J. L.; O'Brien, S. C.; Curl, R. F.; Smalley, R. E. *J. Am. Chem. Soc.* **1988**, *110*, 4464.
(19) Heath, J. R.; Curl, R. F.; Smalley, R. E. *J. Chem. Phys.* **1987**, *87*, 4236.
(20) Yang, S. H.; Pettiette, C. L.; Conceiao, J.; Cheshnovsky, O.; Smalley, R. E. *Chem. Phys. Lett.* **1987**, *139*, 233.
(21) Krätschmer, W.; Fostiropoulos, K.; Huffman, D. R. *Chem. Phys. Lett.* **1990**, *170*, 167.
(22) Kroto, H. W.; McKay, K. *Nature* **1988**, *331*, 328.
(23) Kroto, H. W. *Science* **1988**, *242*, 1139.
(24) Kroto, H. W. *Chem. Brit.* **1990**, *26*, 40.
(25) Frenklach, M.; Ebert, L. B. *J. Phys. Chem.* **1988**, *92*, 561.
(26) Iijima, S. *J. Phys. Chem.* **1987**, *91*, 3466.
(27) Gerhardt, P.; Löffler, S.; Homann, K. H. *Chem. Phys. Lett.* **1987**, *137*, 306.
(28) Léger, A.; d'Hendecourt, L.; Verstraete, L.; Schmidt, W. *Astron. Astrophys.* **1988**, *203*, 145.
(29) Snow, T. P.; Seab, C. G. *Astron. Astrophys.* **1989**, *213*, 291.
(30) Jones, D. H. E. *New Sci.* **1966**, *32*, 245.
(31) Bochvar, D. A.; Gal'pern, E. G. *Dokl. Akad. Nauk. SSSR* **1973**, *209*, 610.
(32) Davidson, R. A. *Theor. Chim. Acta* **1981**, *58*, 193.
(33) Haymet, A. D. J. *Chem. Phys. Lett.* **1985**, *122*, 421.
(34) Haymet, A. D. J. *J. Am. Chem. Soc.* **1986**, *108*, 319.
(35) Hess, B. A., Jr.; Schaad, L. J. *J. Org. Chem.* **1986**, *51*, 3902.
(36) Schmalz, T. G.; Seitz, W. A.; Klein, D. J.; Hite, G. E. *Chem. Phys. Lett.* **1986**, *130*, 203.
(37) Klein, D. J.; Seitz, W. A.; Schmalz, T. G. *Nature* **1986**, *323*, 703.
(38) Klein, D. J.; Schmalz, T. G.; Hite, G. E.; Seitz, W. A. *J. Am. Chem. Soc.* **1986**, *108*, 1301.
(39) Fowler, P. W.; Woolrich, J. *Chem. Phys. Lett.* **1986**, *127*, 78.
(40) Fowler, P. W. *Chem. Phys. Lett.* **1986**, *131*, 444.
(41) Ozaki, M.; Takahashi, A. *Chem. Phys. Lett.* **1986**, *127*, 242.
(42) Haddon, R. C.; Brus, L. E.; Raghavachari, K. *Chem. Phys. Lett.* **1986**, *125*, 459.
(43) Haddon, R. C.; Brus, L. E.; Raghavachari, K. *Chem. Phys. Lett.* **1986**, *131*, 165.
(44) Stone, A. J.; Wales, D. J. *Chem. Phys. Lett.* **1986**, *128*, 501.
(45) Randic, M.; Nikolic, S.; Trinajstic, N. *Croat. Chem. Acta.* **1987**, *60*, 595.
(46) Coulombeau, C.; Rassat, A. *J. Chim. Phys.* **1987**, *84*, 875.
(47) Schmalz, T. G.; Seitz, W. A.; Klein, D. J.; Hite, G. E. *J. Am. Chem. Soc.* **1988**, *110*, 1113.
(48) Aihara, J.; Hosoya, H. *Bull. Chem. Soc. Jpn.* **1988**, *61*, 2657.
(49) Jiang, Y.; Zhang, H. *Theor. Chim. Acta* **1989**, *75*, 279.
(50) Dewar, M. J. S.; de Llano, C. *J. Am. Chem. Soc.* **1969**, *91*, 789.
(51) Newton, M. D.; Stanton, R. E. *J. Am. Chem. Soc.* **1986**, *108*, 2469.

levels with STO-3G[53,57] and double-ζ (DZ)[58,59] basis sets, with additional structural estimates being available from modified Hückel,[41] local-density,[60] and force-field[54,61] approaches. All theoretical methods predict some bond length alternation in C_{60}, typically around 0.07 Å. Whenever comparisons have been made,[34,36,39,44,46,47,51,52,55,58,59] buckminsterfullerene turns out to be more stable than other C_{60} isomers, e.g. graphitene,[51,52] a planar ring,[52] a truncated dodecahedron,[47,55] or planar graphite fragments with dangling bonds.[58,59] Furthermore, buckminsterfullerene appears to be more stable than smaller polyhedral carbon clusters[37,47,51,53] but less stable than some of the larger ones.[37,40,43,47,51,54]

The infrared spectrum of buckminsterfullerene has been predicted from MNDO[62] and from simple force fields,[61,63-65] and a complete set of symmetry coordinates has been reported.[66] The theoretical predictions for the t_{1u} vibrational fundamentals are in reasonable agreement with experiment.[21] Ultraviolet transitions in C_{60} have been computed at the DV-Xα,[67] PPP-CI,[68,69] CNDO/S-CI,[70] and QCFF/PI-CI[71] levels, in the latter case with consideration of Franck–Condon and Jahn–Teller effects. The CNDO/S-CI results[70] are closest to the experimental data[20] for the first allowed band. Likewise, the CNDO/S[70] and LDA-DVM-Xα[72] predictions for the electron affinity of C_{60} agree well with experiment.[19] The available spectroscopic data for C_{60} thus provide strong evidence that this cluster has indeed the icosahedral structure of buckminsterfullerene.

In spite of all the recent activity in this field,[1-72] the experimental and theoretical information on large carbon clusters other than C_{60} is still quite limited. It has indeed been stated[1] "that the present knowledge of C_n molecules and their ions is almost a monotonically decreasing function of n". In this situation a systematic theoretical study would seem to be valuable if it can provide reliable quantitative estimates for the structures, relative stabilities, and other properties of a large number of carbon clusters, and for their variation with cluster size. Previously, in the framework of π electron theory, the most comprehensive investigation[47] covered 54 carbon clusters ($4 \le n \le 240$, no geometry optimization) whereas the largest valence-electron study[51] treated 6 clusters ($24 \le n \le 70$, with geometry optimization). The present paper reports systematic MNDO calculations for 30 carbon clusters ($20 \le m \le 540$, with geometry optimization). It is the main purpose of this paper to present optimized structures for a large class of clusters, to correlate structural data with relative stabilities, and to analyze the calculated MNDO energies in terms of simple models. In addition, the infrared spectra of several stable clusters and the properties of some lithium complexes are predicted.

2. Clusters To Be Studied

All clusters considered are convex polyhedra, have a three-valent σ network, and contain only five-, six-, and possibly seven-membered rings. These rings are more stable than those with 3, 4, or more than 7 atoms because of a larger π stabilization and/or a smaller σ strain.[47] According to some simple combinatoric relations and Euler's theorem, the clusters C_n will have $f_5 = 12 + f_7$ five-membered rings, $f_6 = n/2 - 10 - 2f_7$ six-membered rings, and f_7 seven-membered rings.

The prototype carbon cluster, buckminsterfullerene C_{60}, belongs to the class of Goldberg polyhedra[40,73,74] which have icosahedral symmetry (point group I_h or I) and $n = 20\,(b^2 + bc + c^2)$ vertices where b and c are non-negative integers. When $b - c$ is divisible by 3 the cluster has $60k$ atoms and a closed-shell electronic structure; otherwise it has $60k + 20$ atoms and is expected to be an open-shell species.[40] In the present paper, we study the Goldberg polyhedra with n = 20, 60, 80, 140, 180, 240, and 540 (labeled as clusters of type A) whose optimized structures are

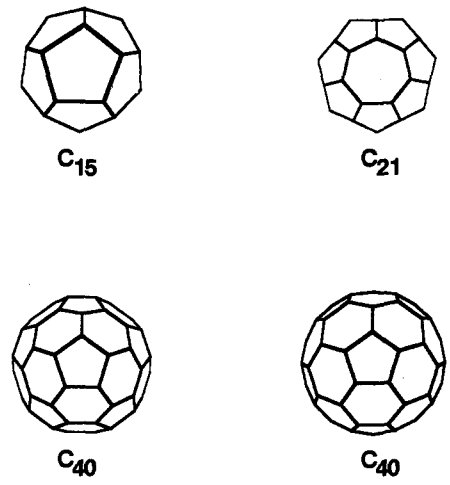

Figure 2. Cluster fragments.

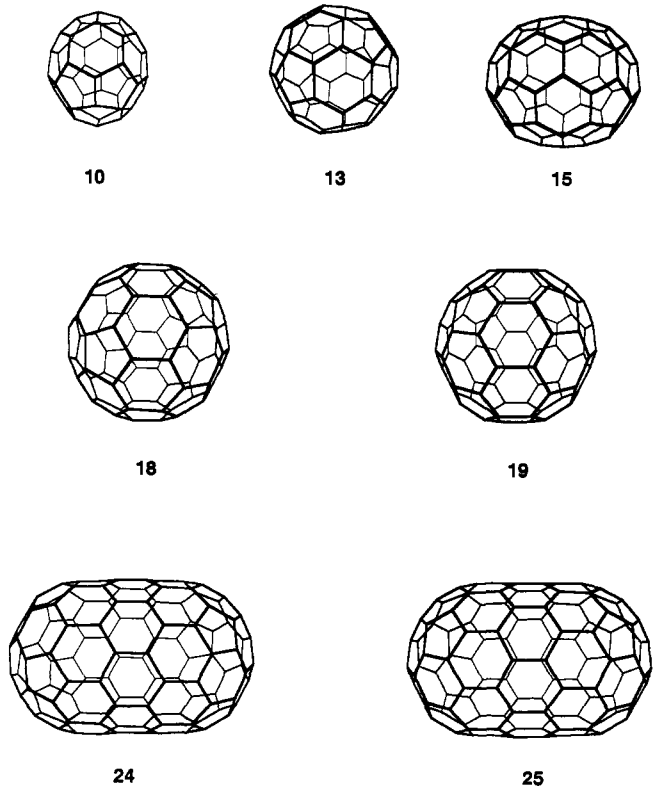

Figure 3. Clusters of type B with topological D_{5h} or D_{5d} symmetry, built from C_{40} fragments. The numbering refers to Tables III and IV.

(52) McKee, M. L.; Herndon, W. C. *J. Mol. Struct. (Theochem)* **1987**, *153*, 75.
(53) Schulman, J. M.; Disch, R. L.; Miller, M. A.; Peck, R. C. *Chem. Phys. Lett.* **1987**, *141*, 45.
(54) Rudziński, J. M.; Slanina, Z.; Togasi, M.; Osawa, E.; Iizuka, T. *Thermochim. Acta* **1988**, *125*, 155.
(55) Shibuya, T.-I.; Yoshitani, M. *Chem. Phys. Lett.* **1987**, *137*, 13.
(56) Marynick, D. S.; Estreicher, S. *Chem. Phys. Lett.* **1986**, *132*, 383.
(57) Disch, R. L.; Schulman, J. M. *Chem. Phys. Lett.* **1986**, *125*, 465.
(58) Lüthi, H. P.; Almlöf, J. *Chem. Phys. Lett.* **1987**, *135*, 357.
(59) Almlöf, J.; Lüthi, H. P. University of Minnesota Supercomputer Institute Report 87/20, Minneapolis, 1987.
(60) Satpathy, S. *Chem. Phys. Lett.* **1986**, *130*, 545.
(61) Cyvin, S. J.; Brendsdal, E.; Cyvin, B. N.; Brunvoll, J. *Chem. Phys. Lett.* **1988**, *143*, 377.
(62) Stanton, R. E.; Newton, M. D. *J. Phys. Chem.* **1988**, *92*, 2141, 5314.
(63) Wu, Z. C.; Jelski, D. A.; George, T. F. *Chem. Phys. Lett.* **1987**, *137*, 291.
(64) Weeks, D. E.; Harter, W. G. *Chem. Phys. Lett.* **1988**, *144*, 366.
(65) Weeks, D. E.; Harter, W. G. *J. Chem. Phys.* **1989**, *90*, 4744.
(66) Brendsdal, E. *Spectrosc. Lett.* **1988**, *21*, 319.
(67) Hale, P. D. *J. Am. Chem. Soc.* **1986**, *108*, 6087.
(68) Kataoka, M.; Nakajima, T. *Tetrahedron* **1986**, *42*, 6437.
(69) Laszlo, I.; Udvardi, L. *Chem. Phys. Lett.* **1987**, *136*, 418.
(70) Larsson, S.; Volossov, A.; Rosén, A. *Chem. Phys. Lett.* **1987**, *137*, 501.
(71) Negri, F.; Orlandi, G.; Zerbetto, F. *Chem. Phys. Lett.* **1988**, *144*, 31.
(72) Rosén, A.; Wästberg, B. *J. Chem. Phys.* **1989**, *90*, 2525.
(73) Goldberg, M. *Tôhoku Math. J.* **1937**, *43*, 104.
(74) Coxeter, H. S. M. In *A spectrum of mathematics*; Butcher, J. C., Ed.; Auckland University Press: Wellington, 1971; pp 98–107.

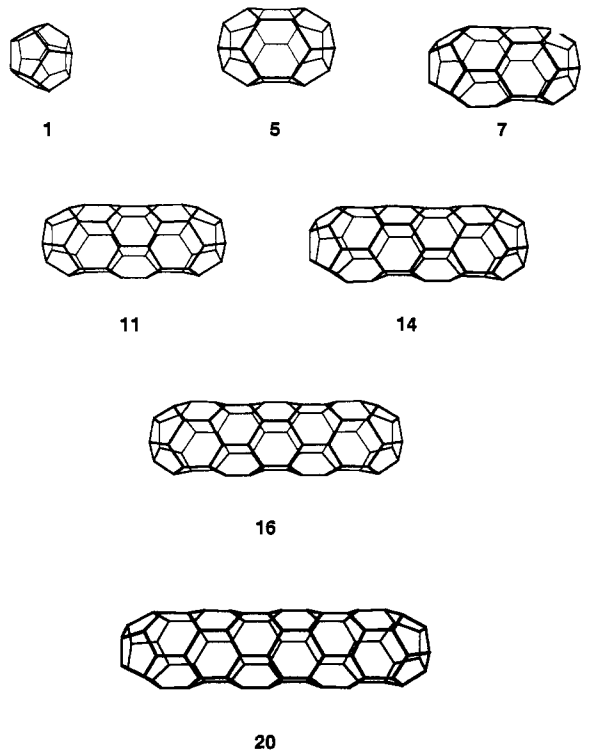

Figure 4. Clusters of type C with topological D_{5h} or D_{5d} symmetry, built from C_{15} fragments. The numbering refers to Tables III and IV.

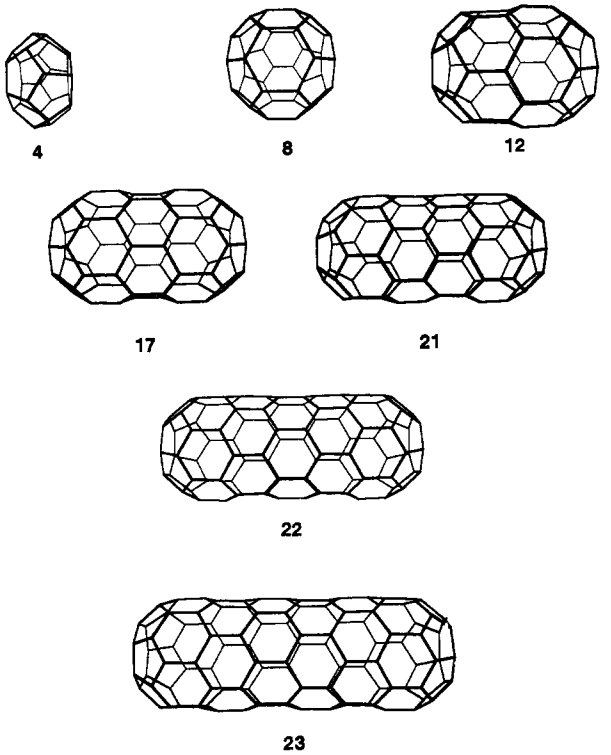

Figure 5. Clusters of type D with topological D_{7h} or D_{7d} symmetry, built from C_{21} fragments. The numbering refers to Tables III and IV.

indicated in Figure 1. Due to icosahedral symmetry the five-membered rings ($f_5 = 12, f_7 = 0$) achieve their maximum possible separation in these clusters.

Other classes of polyhedra may be constructed from fragments which contribute the required number of five- and possibly seven-membered rings. Two such equivalent fragments are suitably oriented and connected by sets of six-membered rings such that a closed polyhedron is formed. The fragments used presently are shown in Figure 2. They have either a C_5 axis (fragments C_{15}, C_{40}) or a C_7 axis (fragment C_{21}). The two C_{40} fragments differ only in the relative positions of the five- and six-membered rings at the periphery. Clusters of type B (topological point group D_{5h} or D_{5d}) can be constructed from the C_{40} fragments (see Figure 3) whereas the C_{15} and C_{21} fragments generate clusters of type C (topological point group D_{5h} or D_{5d}, see Figure 4) and of type D (topological point group D_{7h} or D_{7d}, see Figure 5), respectively. In the construction process, an "overlapping" of the two fragments is allowed (e.g. generation of C_{50} from two C_{40} fragments by sharing 30 common atoms). It should be noted that the procedure described above also generates three Goldberg clusters (C_{20} from C_{15}, C_{60} and C_{80} from C_{40}) which, however, will still generally be considered as type A. The clusters of type B (see Figure 3) contain corannulene moieties and have no fused five-membered rings, with the exception of C_{50}. The curvature is spread rather uniformly over the cage. Therefore, on the basis of previously proposed criteria,[47] these clusters should be rather stable. By contrast, the clusters of types C and D (see Figures 4 and 5) are cigar-shaped and highly anisotropic, and they contain two sets of 6 and 7 fused five-membered rings, respectively. Consequently, they are expected[47] to be quite unstable.

Figure 6 shows the remaining clusters C_n of type E with n = 24, 28, 32, 50, and 120 ($f_5 = 12, f_7 = 0$). They are considered here because they have been suggested to be particularly stable,[40,75] partly in the context of "magic numbers" of cluster stability.[23,24]

3. Semiempirical Calculations

Unless noted otherwise, all calculations were carried out by using the MNDO SCF method with standard parameters.[76] Molecular geometries

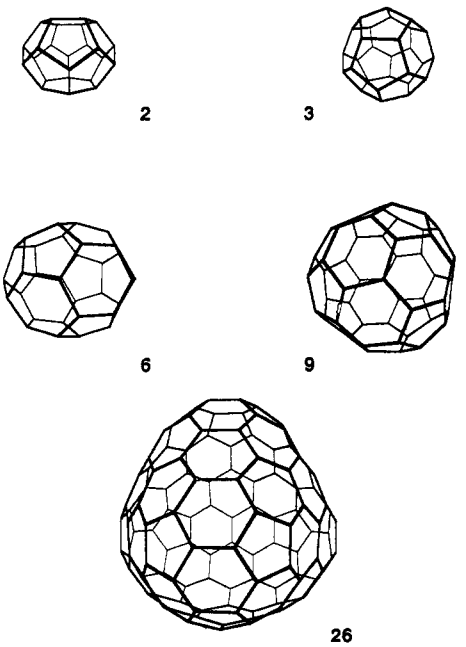

Figure 6. Clusters of type E. The numbering refers to Tables III and IV.

were completely optimized within a given point group by employing the BFGS algorithm.[77-81] A force constant analysis was performed for the majority of stationary points found at the MNDO SCF level (see sections 4D and 4E).

All clusters were treated as closed-shell singlets, with SCF convergence criteria of at least 10^{-5} eV for the energy and 10^{-5} for the diagonal elements of the density matrix. The assumption of a closed-shell electronic structure should not be appropriate for clusters which, due to symmetry, have a zero HOMO–LUMO gap in Hückel approximation.

(75) Kroto, H. W. *Nature* **1987**, *329*, 529.
(76) Dewar, M. J. S.; Thiel, W. *J. Am. Chem. Soc.* **1977**, *99*, 4899.
(77) Broyden, C. G. *J. Inst. Math. Appl.* **1970**, *6*, 76.
(78) Fletcher, R. *Comput. J.* **1970**, *13*, 317.
(79) Goldfarb, D. *Math. Comp.* **1970**, *24*, 23.
(80) Shanno, D. F. *Math. Comp.* **1970**, *24*, 647.
(81) Thiel, W. *J. Mol. Struct.* **1988**, *163*, 415.

Table I. Planar D_{6h} Hydrocarbons C_nH_m ($n = 6k^2$, $m = 6k$)[a,b]

k	n	m	R_{av}, Å	ΔH_f, kcal/mol	E_C, kcal/mol	ϵ_{HOMO}, eV	ϵ_{LUMO}, eV	$\Delta\epsilon$, eV
1	6	6	1.407	21.32	3.37	−9.39	0.37	9.76
2	24	12	1.426	83.06	3.27	−8.08	−1.01	7.07
3	54	18	1.431	183.46	3.14	−7.46	−1.74	5.72
4	96	24	1.433	319.88	3.14	−7.15	−2.14	5.01
5	150	30	1.434	494.05	3.07	−6.88	−2.48	4.40
6	216	36	1.435	703.51		−6.73	−2.68	4.05
∞	∞	0	1.437 (3)		3.0 (2)	−4.7 (5)	−4.7 (5)	0

[a] Average CC bond length R_{av}, heat of formation ΔH_f, energy increment E_C (see text), orbital energies ϵ_{HOMO} and ϵ_{LUMO}, and HOMO–LUMO gap $\Delta\epsilon$. [b] $k = \infty$: extrapolated values for 2D-graphite, with the estimated uncertainty for the last digit given in parentheses.

In such cases, it was indeed found that the closed-shell SCF calculations often encountered problems when carried out for the topological symmetry of the cluster (see section 2). They would either converge to an electron distribution of lower symmetry, or sometimes not converge at all. These problems, whenever they appeared, could be removed by repeating the calculations in a lower geometric symmetry (for details see section 4B). These symmetry reductions led to considerable distortions from the topological symmetry, with maximum changes in the calculated bond lengths of 0.03–0.09 Å and an increase of the calculated HOMO–LUMO gaps of 0.4–1.6 eV. For clusters where such symmetry reductions occur, states of higher multiplicity with similar energy are expected to exist; however, such states are not considered in this study.

In the case of the larger clusters, the definition of the input geometry is non-trivial and merits some comments. It was found advantageous to define the clusters in their topological symmetry by using internal coordinates. For most clusters, these coordinates refer to the origin of the polyhedron and therefore correspond to spherical polar coordinates. In the case of the Goldberg clusters, the internal coordinates were defined with respect to the vertices of the respective icosahedron so that these clusters were built from 12 subunits. When calculations in lower symmetry were necessary (see above), the input for a given Abelian subgroup was done in Cartesian coordinates, and the corresponding input file was generated from that for the topological point group by an automatic computer program. Before starting an MNDO-BFGS optimization, the estimated initial geometry was pre-optimized by minimizing the root-mean-square deviation of all bond lengths from a common standard value of 1.42 Å.

4. Results and Discussion

A. Reference Molecules. Since the carbon clusters have three-valent σ networks with a delocalized π system it is natural to compare their properties with those of graphite. In order to obtain MNDO results for a single sheet of graphite (2D-graphite) by extrapolation, Table I presents MNDO data for a series of six planar D_{6h} hydrocarbons C_nH_m ($n = 6k^2$, $m = 6k$, $k = 1$–6) which are derived from benzene ($k = 1$) by successively adding rings of hexagons ($k = 2$ coronene, etc.). As in analogous ab initio work,[59] the convergence with respect to k is quite good. The average bond length approaches a limiting value of 1.437 (3) Å which agrees with the published value of 1.437 Å from an MNDO solid-state calculation[82] and is slightly larger than the experimental value of 1.421 Å for bulk graphite.[83] It should be noted, however, that even in the largest planar hydrocarbon considered ($k = 6$, $C_{216}H_{36}$) there is still some alternation of the interior CC bond lengths (1.417–1.452 Å) and one distinctly shorter bond of 1.357 Å at the periphery.

In analogy to a previous ab initio study,[59] the MNDO heats of formation in Table I can be expressed by using either atom increments (E_C, E_H) or bond increments (E_{CC}, E_{CH}). According

$$\Delta H_f(k) = 6k^2E_C + 6kE_H = (9k^2 - 3k)E_{CC} + 6kE_{CH} \quad (1)$$

$$E_C(k) = (1/6)[\Delta H_f(k+1)/(k+1) - \Delta H_f(k)/k] = 3E_{CC}(k)/2 \quad (2)$$

to Table I, the increment E_C for a planar carbon system apparently converges to a value of 3.0 (2) kcal/mol which is close to a similar estimate of 2.5 kcal/mol from ab initio 6-31G* SCF calculations.[84]

Table II. Comparison of MNDO, ab Initio SCF, and Experimental Data for Corannulene $C_{20}H_{10}$ and Buckminsterfullerene C_{60}

molecule	property[a]	MNDO	ab initio[b]	experiment[c]
$C_{20}H_{10}$	R_a (Å)	1.443	1.423	1.413
	R_b (Å)	1.393	1.361	1.391
	R_c (Å)	1.458	1.462	1.440
	R_d (Å)	1.394	1.363	1.402
	θ_A (deg)	7.7		8.2
	θ_B (deg)	3.0		3.8
	ΔH_f (kcal/mol)	134.3	123.4[d]	
C_{60}	R_a (Å)	1.474	1.453[e]	
	R_b (Å)	1.400	1.369[e]	
	ΔE^c (kcal/mol)[f]	11.5	11	
	IP (eV)[g]	8.95	7.92	6.4–7.9[h]
	EA (eV)[g]	2.68	0.80	2.6–2.8
	ν_i (cm^{-1})[i]	1628 s		1429 s
		1352 ms		1183 w
		718 w		577 w
		578 m		528 m

[a] See supplementary material for the definition of bond lengths R and POAV angles θ. [b] Unless noted otherwise: $C_{20}H_{10}$, STO-3G results from ref 84; C_{60}, DZ results from refs 58 and 59. [c] X-ray data for $C_{20}H_{10}$ from ref 90, spectroscopic data assigned to C_{60} from refs 8, 20, and 21. [d] Reference 84, using energy increments from fitting ab initio SCF total energies to experimental heats of formation of benzenoid hydrocarbons. Analogous 6-31G*//STO-3G result: 117.2 kcal/mol. [e] STO-3G (ref 57): R_a = 1.465 Å, R_b = 1.376 Å. [f] Energy per atom relative to 2D-graphite. [g] Ionization potential (IP) and electron affinity (EA) calculated by the ΔE_{SCF} procedure at the optimized geometry of C_{60}. [h] Experimental value probably at the upper end of this range. [i] Wavenumbers and relative intensities (standard notation) for the infrared-active vibrational modes (t_{1u}).

Experimentally, E_C is zero for bulk graphite, by definition, and around 1.5–2.0 kcal/mol for a single sheet of 2D-graphite, according to empirical estimates[85,86] for the van der Waals interactions between the graphite layers. Hence, MNDO overestimates E_C by about 1.0–1.5 kcal/mol which is consistent with the known errors of MNDO heats of formation for large benzenoid hydrocarbons.[84,87]

The HOMO and LUMO orbital energies in Table I converge rather slowly toward a value of −4.7 (5) eV which would correspond to the work function for 2D-graphite. This may be compared with an analogous ab initio value[59] of −4 eV and with an experimental value[88] of 4.8 eV for the work function of bulk graphite.

In order to check the accuracy of MNDO for carbon clusters, Table II reports MNDO, ab initio SCF, and experimental data for corannulene $C_{20}H_{10}$ and buckminsterfullerene C_{60}. The known corannulene molecule[89,90] is relevant in this connection because its carbon skeleton appears in all clusters of types A and B (except C_{20}). Compared with experiment MNDO predicts the CC bond lengths of corannulene in the correct order, with a mean absolute error of less than 0.02 Å, while the calculated angles show deviations of less than 1°. In the case of C_{60}, the true bond lengths

(82) Lee, Y.-S.; Kertesz, M. *J. Chem. Phys.* **1988**, *88*, 2609.
(83) Gmelin, *Handbuch der Anorganischen Chemie*, 8th ed.; Verlag Chemie: Weinheim, 1968; Vol. 14B/2, p 413.
(84) Schulman, J. M.; Peck, R. C.; Disch, R. L. *J. Am. Chem. Soc.* **1989**, *111*, 5675.
(85) Benson, S. W. *Thermochemical Kinetics*; Wiley: New York, 1976.
(86) Girifalco, L. A.; Lad, R. A. *J. Chem. Phys.* **1956**, *25*, 693.
(87) Stewart, J. J. P. *J. Comput. Chem.* **1989**, *10*, 221.
(88) Willis, R. F.; Feuerbacher, B.; Fitton, B. *Phys. Rev. B.* **1971**, *4*, 2441.
(89) Barth, W. E.; Lawton, R. G. *J. Am. Chem. Soc.* **1971**, *93*, 1730.
(90) Hanson, J. C.; Nordman, C. E. *Acta Cryst. B* **1976**, *32*, 1147.

Table III. Topological and Structural Data[a] for Carbon Clusters C_n

k	n	type[b]	point group[c]	N_G[c]	R_{av}, Å	R_{min}, Å	R_{max}, Å	θ_{av}, deg	θ_{min}, deg	θ_{max}, deg	$\sum\theta_i^2$, rad^2	$\sum\tau_i^2$, rad^2	$\sum\alpha_i^2$, rad^2
1	20	A[b]	I_h/C_1	1/54	1.474	1.408	1.518	20.90	20.29	21.54	2.663	22.92	2.655
2	24	E	D_{6d}/C_1	4/66	1.470	1.388	1.531	19.01	17.42	20.59	2.659	23.04	2.743
3	28	E	T_d/C_1	5/78	1.465	1.392	1.548	17.39	16.14	20.17	2.587	22.57	2.690
4	28	D	D_{7d}/C_1	4/78	1.470	1.379	1.545	17.75	14.27	21.18	2.766	24.00	3.814
5	30	C	D_{5h}/C_{2v}	6/23	1.465	1.398	1.513	17.23	12.68	22.15	2.811	24.42	2.780
6	32	E	C_3/C_1	30/90	1.461	1.379	1.532	16.24	14.07	19.27	2.591	22.68	2.776
7	40	C	D_{5d}	8	1.465	1.373	1.508	15.41	9.62	20.73	3.105	27.06	3.036
8	42	D	D_{7h}/C_s	6/60	1.455	1.399	1.522	13.97	12.97	15.04	2.500	22.05	3.482
9	50	E	D_3	25	1.452	1.387	1.497	12.87	10.10	15.00	2.544	22.50	2.750
10	50	B	D_{5h}	9	1.453	1.389	1.485	12.86	11.50	15.25	2.544	22.49	2.680
11	50	C	D_{5h}/C_{2v}	10/39	1.460	1.400	1.506	14.45	9.18	22.39	3.483	30.37	3.181
12	56	D	D_{7d}/C_1	8/162	1.452	1.400	1.516	12.38	8.00	15.72	2.738	24.18	3.533
13	60	A[b]	I_h	2	1.449	1.400	1.474	11.64	11.64	11.64	2.477	21.98	2.632
14	60	C	D_{5d}	12	1.462	1.373	1.506	13.61	9.70	20.72	3.718	32.51	3.639
15	70	B	D_{5h}	12	1.448	1.389	1.484	10.82	8.87	11.97	2.523	22.43	2.735
16	70	C	D_{5h}	14	1.461	1.373	1.506	13.10	9.69	20.73	4.024	35.24	3.937
17	70	D	D_{7h}/C_{2v}	10/54	1.450	1.405	1.513	11.39	6.38	15.89	3.002	26.53	3.566
18	80	A[b]	I_h/C_1	3/234	1.447	1.400	1.487	10.06	9.30	10.42	2.472	22.02	2.841
19	80	B	D_{5h}/C_s	14/117	1.447	1.366	1.493	10.08	8.67	11.20	2.487	22.14	2.865
20	80	C	D_{5d}	16/63	1.456	1.410	1.506	12.82	9.54	22.39	4.408	38.61	3.940
21	84	D	D_{7d}/C_1	12/123	1.449	1.408	1.512	10.72	6.56	15.93	3.233	28.60	3.654
22	98	D	D_{7h}/C_s	14/144	1.448	1.410	1.511	10.23	6.75	15.92	3.462	30.64	3.740
23	112	D	D_{7d}/C_1	16/330	1.449	1.382	1.528	9.84	6.26	15.43	3.672	32.53	3.969
24	120	B	D_{5d}/C_s	21/183	1.445	1.382	1.500	8.46	4.49	10.75	2.793	24.90	2.934
25	120	B	D_{5h}/C_{2v}	21/92	1.445	1.378	1.487	8.45	4.89	10.65	2.792	24.89	2.914
26	120	E	T_d	17	1.445	1.392	1.473	8.43	4.87	12.14	2.857	25.44	2.893
27	140	A	I/C_1	7/414	1.444	1.380	1.486	7.68	5.95	9.62	2.607	23.30	3.358
28	180	A	I_h	6	1.443	1.396	1.463	6.83	5.02	9.70	2.790	24.93	3.335
29	240	A	I_h	7	1.442	1.394	1.465	5.95	4.22	9.67	2.947	26.35	3.427
30	540	A	I_h	15	1.440	1.395	1.458	4.00	2.24	10.31	3.625	32.41	3.167

[a] Number of independent geometrical variables (N_G); average, minimum, and maximum bond lengths (R_{av}, R_{min}, R_{max}); average, minimum, and maximum POAV angles (θ_{av}, θ_{min}, θ_{max}); sum of squares of n POAV angles θ_i, n out-of-plane angles τ_i, and $3n$ deviations $\alpha_i = \alpha_{CCC} - 2\pi/3$ of CCC bond angles from 120°. [b] See text. Cluster 1 can also be assigned to type C, and clusters 13 and 18 to type B. [c] If there are two entries, the first one refers to the topological group, and the second one to the lower point group found in the geometry optimization.

are expected to be close to the average of those calculated from MNDO and ab initio SCF (DZ basis),[58,59] judging from the errors of these methods for aromatic compounds. The theoretical energies per atom in C_{60} (relative to 2D-graphite) from MNDO and ab initio DZ-SCF calculations[59] are within 1 kcal/mol of each other. It should be noted, however, that the addition of polarization functions is estimated[59] to decrease the ab initio value in Table II by about 2 kcal/mol which is consistent with recent 6-31G* results.[84,91] Finally, the MNDO predictions for the spectroscopic properties of C_{60} are of the expected accuracy.[51,87,92-94]

In summary, the results in Tables I and II indicate that MNDO should describe carbon clusters reasonably well. It is expected that MNDO may tend to overestimate bond lengths by 0.01–0.02 Å, and heats of formation per carbon atom by 1–2 kcal/mol, but trends for different clusters should be realistic. In addition we note that AM1[95] and PM3[87] yield results similar to MNDO in test calculations for selected clusters C_n ($60 \le n \le 240$), with small systematic deviations in the computed bond lengths and heats of formation per atom (e.g. AM1 + 1.7 (1) kcal/mol).

B. Structure of the Clusters. The optimized geometries of the clusters (see Figures 1–6) and the reference molecules (see section 4A) are given in full detail in the supplementary material. Table III summarizes the most important structural data. Each cluster C_n is identified by a running index k, the number of atoms n, its type (A–E, see section 2), the point group, and the number of independent geometrical variables N_G, with two entries in the latter two cases if symmetry reduction occurs (see section 3).

The average bond lengths R_{av} decrease regularly with increasing n, from 1.474 (n = 20) to 1.440 Å (n = 540), and approach the limiting value of 1.437 Å for 2D-graphite from above. The extent of bond alternation is indicated by the minimum and maximum bond lengths (R_{min}, R_{max}). The curvature at a given atom i may be measured with the help of the π orbital axis vector (POAV)[96] which is geometrically defined such that it has equal angles β_i with the three bonds of that atom. The corresponding POAV angle is then defined as $\theta_i = \beta_i - \pi/2$ (i.e. $\theta_i = 0$ in the planar case). As expected, the average POAV angles θ_{av} decrease regularly with increasing cluster size (similarly for θ_{min}). The maximum POAV angles θ_{max} are always associated with atoms in five-membered rings. For larger systems ($n > 50$), they assume typical values for clusters of a given type, i.e. 10–12° (types A, B), 21–22° (type C), and 15–16° (type D). The high values for types C and D reflect the strong curvature at the ends of these cigar-shaped structures (see Figures 4 and 5).

Under certain simplifying assumptions it has been shown[47] that the sum of the squares of the POAV angles should be nearly constant for spheroidal clusters

$$\Sigma\theta_i^2 \approx 4\pi/(3\sqrt{3}) = 2.418 \qquad (3)$$

As a consequence of this "curvature conservation" the nonplanar σ strain has been assumed to be independent of the cage.[47] The results in Table III show that this hypothesis holds with an accuracy of 20% for most clusters of types A, B, and E (except C_{240}, C_{540}), but generally not for clusters of types C and D. Similar conclusions apply to the sum $\Sigma\tau_i^2$ where the out-of-plane angle $\tau_i = 3 \sin \theta_i$ (i.e. $\tau_i \approx 3\theta i$ for small θ_i) has been defined in accordance with an empirical force field for aromatic hydrocarbons.[97] The last column in Table III lists the sums $\Sigma\alpha_i^2$ where α_i is the deviation of a CCC angle from its ideal sp^2 value of $2\pi/3$. Since each cluster contains at least 12 pentagons this sum must be at least 2.632 (i.e. the value for buckminsterfullerene). It has been argued[47] that this value should be appropriate for all polyhedra

(91) Fowler, P. W.; Lazzeretti, P.; Zanasi, R. *Chem. Phys. Lett.* **1990**, *165*, 79.
(92) Dewar, M. J. S.; Thiel, W. *J. Am. Chem. Soc.* **1977**, *99*, 4907.
(93) Dewar, M. J. S.; Rzepa, H. S. *J. Am. Chem. Soc.* **1978**, *100*, 784.
(94) Dewar, M. J. S.; Ford, G. P.; McKee, M. L.; Rzepa, H. S.; Thiel, W.; Yamaguchi, Y. *J. Mol. Struct.* **1978**, *43*, 135.
(95) Dewar, M. J. S.; Zoebisch, E. G.; Healy, E. F.; Stewart, J. J. P. *J. Am. Chem. Soc.* **1985**, *107*, 3902.
(96) Haddon, R. C.; Scott, L. T. *Pure Appl. Chem.* **1986**, *58*, 137.
(97) Cyvin, B. N.; Neerland, G.; Brunvoll, J.; Cyvin, S. J. *Z. Naturforsch.* **1980**, *35a*, 731.

Table IV. Heats of Formation and Related Data for Carbon Clusters C_n[a,b]

k	n	type[c]	ΔH_f	ΔH_f^c	ΔH_f^{rel}	ΔE_π	ΔE_τ	ΔE_α	m_C	$-\epsilon_{HOMO}$	$-\epsilon_{LUMO}$	$\Delta\epsilon$
1	20	A	825.2	41.26	765.2	247	538	166	1.4708	8.85	2.86	5.99
2	24	E	850.2	35.42	778.2	267	537	171	1.4758	9.14	2.76	6.38
3	28	E	871.0	31.11	787.0	271	523	166	1.4804	8.84	3.20	5.64
4	28	D	995.9	35.57	911.9	306	560	237	1.4807	8.55	3.24	5.31
5	30	C	944.6	31.49	854.6	304	566	172	1.4960	8.75	3.17	5.58
6	32	E	874.2	27.32	778.2	252	523	171	1.5201	8.82	3.34	5.48
7	40	C	1133.9	28.35	1013.9	401	627	188	1.5100	9.09	3.94	5.15
8	42	D	941.3	22.41	815.3	268	504	212	1.5146	8.51	3.32	5.19
9	50	E	929.1	18.58	779.1	249	512	167	1.5414	7.95	4.00	3.95
10	50	B	922.2	18.44	772.2	256	513	163	1.5391	8.48	3.27	5.21
11	50	C	1300.1	26.00	1150.1	501	699	195	1.5197	7.89	3.60	4.29
12	56	D	1095.6	19.56	927.6	323	551	214	1.5317	8.17	3.73	4.44
13	60	A	869.3	14.49	689.3	230	498	159	1.5527	9.13	2.56	6.57
14	60	C	1468.8	24.48	1288.8	584	750	224	1.5270	8.87	4.08	4.79
15	70	B	939.3	13.42	729.3	247	508	165	1.5545	8.67	2.84	5.83
16	70	C	1636.6	23.38	1426.6	674	812	242	1.5327	8.75	4.11	4.64
17	70	D	1242.1	17.74	1032.1	394	602	216	1.5410	7.76	4.16	3.60
18	80	A	1060.2	13.25	820.2	276	498	171	1.5438	8.38	3.98	4.40
19	80	B	1030.2	12.88	790.2	262	501	173	1.5473	8.15	3.88	4.27
20	80	C	1849.5	23.12	1609.5	773	884	240	1.5373	6.26	5.16	1.10
21	84	D	1382.9	16.46	1130.9	460	648	221	1.5470	7.47	4.49	2.98
22	98	D	1523.4	15.55	1229.4	526	694	226	1.5512	7.15	4.80	2.35
23	112	D	1642.7	14.67	1306.7	598	737	240	1.5543	7.74	3.80	3.94
24	120	B	1301.0	10.84	941.0	362	561	176	1.5553	7.86	4.34	3.52
25	120	B	1293.0	10.78	933.0	356	561	175	1.5561	7.08	4.98	2.10
26	120	E	1201.9	10.02	841.9	338	573	174	1.5633	8.46	2.78	5.68
27	140	A	1299.9	9.28	879.9	306	524	202	1.5590	7.83	3.93	3.90
28	180	A	1392.4	7.74	852.4	330	560	200	1.5670	8.53	2.96	5.57
29	240	A	1595.5	6.65	875.5	366	591	205	1.5689	8.22	3.04	5.18
30	540	A	2580.2	4.78	960.2	575	726	189	1.5721	7.69	3.30	4.39

[a] Heat of formation: total (ΔH_f), per atom (ΔH_f^c), and relative to n atoms of 2D-graphite (ΔH_f^{rel}); contributions to ΔH_f^{rel} arising from diminished π interaction (ΔE_π), out-of-plane strain (ΔE_τ), and in-plane strain (ΔE_α), see text; Hückel energies per atom (m_C); negative MNDO orbital energies $-\epsilon_{HOMO}$, $-\epsilon_{LUMO}$, and HOMO–LUMO gap $\Delta\epsilon$. [b] In kcal/mol, except m_C (in units of β) and orbital energies (in eV). [c] See text and footnote *b* of Table III.

with 12 pentagons which would imply a constant in-plane σ strain from bending. As can be seen from Table III, this assumption holds with an accuracy of 20% for most clusters C_n of types A, B, and E (except $n \geq 140$) but generally not for clusters of type C, whereas it does not apply to clusters of type D with 14 pentagons and 2 heptagons.

The principles underlying the structures of large carbon clusters can be inferred from the optimized geometry of C_{540} which is drawn to scale in Figure 1 (see supplementary material for details). In striking similarity to previously proposed models,[22-24] the MNDO structure of C_{540} is not spherical but icosahedral. The curvature is localized in the 12 pentagons with POAV angles of 10.3°. These angles drop to 5.7° for the adjacent carbon atoms and to 2.2–3.7° for the remaining atoms (close to planarity). Likewise, the shortest CC distance of 1.395 Å refers to the radial bond at the pentagons, while the remaining bond lengths are in the same range (1.414–1.458 Å) as the interior bonds in the planar hydrocarbon $C_{216}H_{36}$ (1.417–1.452 Å). Clearly the MNDO structure of C_{540} can qualitatively be described as graphite segments joined by 12 pentagonal defects which are required for the three-dimensional closure of the cage.

C. Stability of the Clusters. Table IV lists the calculated MNDO heats of formation, contributions to relative energies in an energy partitioning scheme (see below), Hückel resonance energies, and MNDO orbital energies. In columns 4–6 the MNDO heats of formation are given for the cluster (ΔH_f), per carbon atom ($\Delta H_f^c = \Delta H_f/n$), and for the cluster relative to n carbon atoms in 2D-graphite ($\Delta H_f^{rel} = \Delta H_f - nE_c$, $E_c = 3$ kcal/mol, see section 4A). ΔH_f^c is the quantity which determines the thermodynamic stability of clusters of different size. It is obvious from Table IV that, in an overall perspective, ΔH_f^c decreases with increasing cluster size and approaches the limiting value of 3.0 kcal/mol for 2D-graphite from above. On a per-atom basis, C_{540} is predicted to be only 1.8 kcal/mol less stable than 2D-graphite so that it would seem to constitute an energetically feasible allotropic form of carbon.

In view of the tendency to avoid curvature and to prefer planar graphite segments in large clusters (see above) it is natural to correlate the thermodynamic stability with the average curvature of the cluster which can be characterized[47] by $\Sigma\theta_i^2/n$. A linear regression analysis

$$\Delta H_f^c = [a\Sigma\theta_i^2/n + b] \text{ kcal/mol} \quad (4)$$

using the data for all 30 clusters in Tables III and IV yields $a = 298.5 \pm 7.9$ and $b = 4.0 \pm 0.5$, with a correlation coefficient of 0.990 and a standard error of 1.3 kcal/mol. The plot of this regression in Figure 7 shows that clusters with many fused five-membered rings (e.g. types C and D) are less stable than expected from this correlation, presumably due to local antiaromatic pentalene subunits. Excluding all clusters with fused pentagons, a linear regression for the remaining 11 clusters leads to $a = 290.3 \pm 19.2$ and $b = 3.4 \pm 0.5$, with a correlation coefficient of 0.980

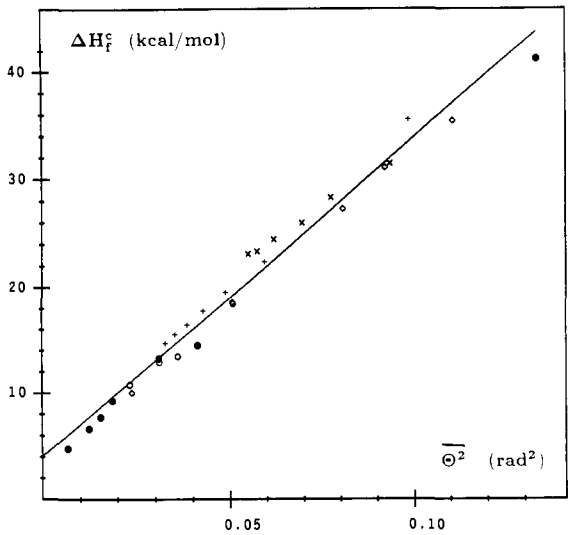

Figure 7. MNDO heat of formation per atom (ΔH_f^c) plotted versus the average squared POAV angle ($\overline{\theta^2}$). Cluster types: A (●), B (○), C (×), D (+), E (◇).

and a standard error of 0.6 kcal/mol. In this second regression the limiting value of 3.0 ± 0.2 kcal/mol for 2D-graphite (all $\theta_i = 0$) is reproduced. It seems remarkable that simple correlations as in eq 4 allow a reasonably accurate estimate of thermodynamic stability from structural data.

Many previous studies[31-49] have discussed the stability of carbon clusters in the framework of π electron theory. In Hückel approximation the total π energy of a cluster (label C) and of a 2D-graphite segment with n atoms (label G) is given by

$$E(\mathrm{C}) = n(\alpha + m_{\mathrm{C}}\beta_{\mathrm{C}}),\ m_{\mathrm{C}} \text{ see Table IV} \quad (5)$$

$$E(\mathrm{G}) = n(\alpha + m_{\mathrm{G}}\beta_{\mathrm{G}}),\ m_{\mathrm{G}} = 1.5746 \text{ (ref 47)} \quad (6)$$

Assuming $\beta = \beta_{\mathrm{C}} = \beta_{\mathrm{G}}$ it is customary to define a relative resonance energy per π electron, $D_{\mathrm{REPE}} = (m_{\mathrm{C}} - m_{\mathrm{G}})\beta$. We find, however, that this quantity does not correlate well with ΔH_f^{c}. For a more realistic description at the Hückel level, a curvature correction for β_{C} should be introduced, in the spirit of the POAV/3D HMO model[42,43,98]. We define an average MNDO $\pi\pi$ overlap integral in the cluster by

$$S_{\mathrm{C}} = \langle S_{ij} \rangle = \langle \cos\theta_i \cos\theta_j \cos\phi_{ij} [S_{\pi\pi}(R_{ij})] \rangle \quad (7)$$

where θ_i and θ_j are the POAV angles for neighboring atoms, ϕ_{ij} is the dihedral angle between the corresponding POAV vectors, and $S_{\pi\pi}(R_{ij})$ is the standard MNDO $\pi\pi$ overlap integral for the CC bond length R_{ij}. Denoting the MNDO $\pi\pi$ overlap in 2D-graphite (R_{G} = 1.437 Å) by $S_{\mathrm{G}} = S_{\pi\pi}(R_{\mathrm{G}})$ we assume $\beta_{\mathrm{C}} = (S_{\mathrm{C}}/S_{\mathrm{G}})\beta_{\mathrm{G}}$. The curvature-corrected resonance energy per π electron (evaluated at the MNDO optimized geometry) then becomes

$$D_{\mathrm{CREPE}} = [(S_{\mathrm{C}}/S_{\mathrm{G}})m_{\mathrm{C}} - m_{\mathrm{G}}]\beta_{\mathrm{G}} \quad (8)$$

A linear regression analysis for all 17 clusters of types A, B, and E yields

$$\Delta H_f^{\mathrm{c}} = [cD_{\mathrm{CREPE}}/\beta_{\mathrm{G}} + d] \text{ kcal/mol} \quad (9)$$

with c = 101.4 ± 1.7, d = 2.1 ± 0.3, a correlation coefficient of 0.998, and a standard error of 0.7 kcal/mol. An analogous regression analysis for all 30 clusters leads to unsatisfactory results (maximum error of almost 6 kcal/mol) which is not surprising since the clusters of types C and D are very anisotropic (with $\theta_{\max}$ values similar to a tetrahedral configuration, see Table III) and contain structural fragments which are not well described at the Hückel level. Nevertheless, the success of the correlation in eq 9 for cluster types A, B, and E demonstrates that curvature-corrected Hückel calculations can reproduce the relative stabilities of carbon clusters without too many fused five-membered rings.

Applying these considerations in the MNDO framework, the total π destabilization energy of a given cluster C_n relative to 2D-graphite may be expressed quantitatively as $\Delta E_\pi = nD_{\mathrm{CREPE}}$ where D_{CREPE} is evaluated according to eq 9 with the MNDO value of β_{G} = −32.48 kcal/mol. A comparison of ΔE_π with the total destabilization energy $\Delta H_f^{\mathrm{rel}}$ in Table IV indicates that the diminished π interaction accounts for typically 35–40% of the total destabilization and that the rest must come from σ strain, in this model.

As an alternative approach to energy partitioning it is possible to apply simple force field arguments[47] and to identify the two major sources of destabilization as out-of-plane (τ) and in-plane (α) bending. The force constants k_τ and k_α may be taken from

$$\Delta E_\tau = (k_\tau/2)\Sigma\tau_i^2 \quad (10)$$

$$\Delta E_\alpha = (k_\alpha/2)\Sigma\alpha_i^2 \quad (11)$$

the literature. We have chosen k_τ = 21.59 kcal mol^{-1} rad^{-2} $(R_{\mathrm{av}}/\text{Å})^2$ and k_α = 57.57 kcal mol^{-1} rad^{-2}$(R_{\mathrm{av}}/\text{Å})^2$ from a force field[97,99] which has been designed to describe the vibrations in aromatic molecules and which predicts reasonable vibrational frequencies for buckminsterfullerene.[61] Table IV lists the quantities ΔE_τ and ΔE_α evaluated from these force constants and from the structural data in Table III. These two contributions are indeed found to represent the major part of the total destabilization energy $\Delta H_f^{\mathrm{rel}}$ since their sum $\Delta E_\tau + \Delta E_\alpha$ usually amounts to 85 ± 10% of $\Delta H_f^{\mathrm{rel}}$, with typically 20 ± 5% from ΔE_α and 65 ± 5% from ΔE_τ (note that ΔE_τ includes ΔE_π, by definition). To illustrate the results of this partitioning scheme the percentage contributions of ΔE_α, $\Delta E_\alpha + \Delta E_\pi$, and $\Delta E_\alpha + \Delta E_\tau$ to $\Delta H_f^{\mathrm{rel}}$ are plotted in Figure 8 for all clusters of types A, B, and E.

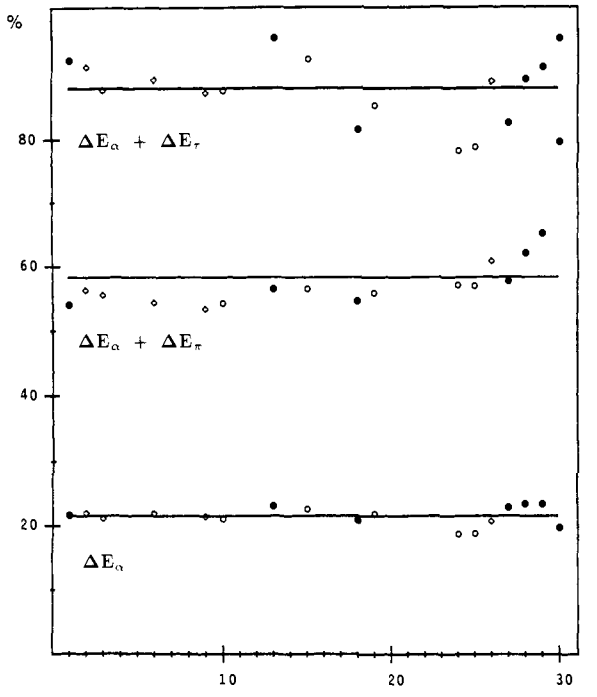

Figure 8. Percentage contributions of ΔE_α (bottom), $\Delta E_\alpha + \Delta E_\pi$ (middle), and $\Delta E_\alpha + \Delta E_\tau$ (top) to the total destabilization $\Delta H_f^{\mathrm{rel}}$. Cluster types: A (●), B (○), E (◇).

It is instructive to compare the total destabilization energies $\Delta H_f^{\mathrm{rel}} = \Delta H_f - nE_{\mathrm{c}}$ of different clusters C_n relative to n atoms of 2D-graphite (see Table IV). MNDO predicts by far the lowest value for buckminsterfullerene C_{60} (k = 13; 689 kcal/mol) followed by the most stable C_{70} isomer (k = 15; 729 kcal/mol) and then a group of smaller clusters (k = 1–3, 6, 9, 10; 765–787 kcal/mol) which includes those with suggested "magic number" stability[23,24] (C_{24}, C_{28}, C_{32}, C_{50}). On the other hand, particularly high values of $\Delta H_f^{\mathrm{rel}} > 1000$ kcal/mol always belong to clusters of types C and D. It should be stressed, however, that the thermodynamic stability of a cluster is governed by ΔH_f^{c} and not by $\Delta H_f^{\mathrm{rel}}$. Significant differences in $\Delta H_f^{\mathrm{rel}}$ can easily be reversed when evaluating relative stabilities on a per-atom basis through division by n.

Another distinction between clusters of types A–D concerns the bond energy increments E_{CC}. Large clusters of a given type differ, by construction, only in the number of CC bonds which simultaneously belong to two six-membered rings. Increments E_{CC} for these bonds can thus be derived easily from ΔH_f (see Table IV) which leads to the following values (in kcal/mol): A, 2.0 ± 0.2; B, 4.1 ± 0.5; C, 11.0 ± 1.0; D, 6.0 ± 1.0. The value for clusters of type A is identical with that for 2D-graphite (see section 4A, eq 2 and Table I) which confirms again that large Goldberg clusters such as C_{540} can be regarded to contain graphite segments. On the other hand, the growth of the cigar-shaped clusters of types C and D cannot proceed toward graphite segments because each new belt of hexagons is strongly curved, particularly for type C (see Figures 4 and 5).

A previous study[47] has proposed six criteria for the stability of carbon clusters: (1) three-valent σ network, (2) cage homeomorphic to a sphere, (3) five- and six-sided rings only, (4) higher

(98) Haddon, R. C. *J. Am. Chem. Soc.* **1986**, *108*, 2837.
(99) Bakke, A.; Cyvin, B. N.; Whitmer, J. C.; Cyvin, S. J.; Gustavsen, J. E.; Klaeboe, P. *Z. Naturforsch.* **1979**, *34a*, 579.

symmetry, (5) no abutting five-sided rings, and (6) curvature spread uniformly over the cage. The last three criteria may be checked against the present MNDO results. Criterion 4 is confirmed for highly symmetric structures if they correspond to closed-shell species (e.g. see the icosahedral clusters of type A with n = 60, 180, 240, 540); if this is not true, however, the closed-shell singlets distort to unsymmetric structures (e.g. see the C_{140} cluster of type A with point group C_1) which, of course, does not exclude that highly symmetric stable structures may exist for higher multiplicities (not studied presently). Criterion 5 is confirmed generally: Clusters with many abutting five-membered rings are always calculated to be very unstable (see types C and D). The destabilizing effect of one pair of fused pentagons may be estimated to be approximately 7 kcal/mol, from a comparison of the heats of formation of the two most stable C_{50} isomers (k = 9, $\sum\theta_i^2$ = 2.544, 6 such pairs, and k = 10, $\sum\theta_i^2$ = 2.544, 5 such pairs, see Tables III and IV), which is close to the resonance destabilization of 6.5 kcal/mol obtained for pentalene.[100] Criterion 6 is not supported generally: Although highly anisotropic clusters (e.g. types C and D) are indeed found to be unstable, the curvature in the large icosahedral clusters of type A is not spread uniformly, but localized around the pentagons due to the preference for planar graphite segments (see C_{540}, Figure 1 and section 4B). It is interesting to note that the previous study[47] has assumed the relative stability of various clusters to depend dominantly on π resonance energies which, according to our partitioning scheme, account for typically only 35–40% of the total destabilization. Nevertheless, the two investigations still lead to many similar conclusions since the total destabilization energy and the π electron contribution often show similar trends, at least for clusters of types A, B, and E (see above).

The last three columns in Table IV list MNDO orbital energies and HOMO–LUMO gaps. On the basis of Koopmans' theorem the negative HOMO and LUMO energies approximate the ionization potentials and electron affinities of the clusters, respectively. While the former are expected to be overestimated (by about 1 eV)[51,87] the latter may be realistic.[93] The observed electron affinities[20] for C_{50} (≈3.1 eV), C_{60} (≈2.7 eV), and C_{70} (≈2.8 eV) are indeed close to the MNDO predictions for the most stable isomers of these clusters (k = 10, 13, 15). The calculated HOMO–LUMO gaps are generally quite low for those species where symmetry reduction occurs (see section 3 and Table III) while they show the expected general decrease with increasing cluster size for the remaining molecules (see e.g. type A: k = 13, 28–30).

D. Infrared Spectra. Force constant calculations have been carried out for all clusters up to 70 atoms (k = 1–17), the most stable C_{80} and C_{120} isomers (k = 18, 19, 26), C_{180}, and C_{240} (k = 28, 29). All these clusters are minima on the MNDO SCF potential surface. A recent report[21] on the experimental infrared spectrum of buckminsterfullerene prompts us to summarize some results of these force constant calculations, full details being given elsewhere.[101]

Figure 9 shows the predicted infrared spectra of the most stable C_{50}, C_{60} (see ref 62), and C_{70} clusters (k = 10, 13, 15) where the lengths of the sticks in the diagrams are proportional to the calculated infrared intensities. Due to symmetry the number of infrared-allowed vibrational fundamentals is small: 22 for C_{50} (7 a_2'' + 15 e_1'), 4 for C_{60} (4 t_{1u}), and 31 for C_{70} (10 a_2'' + 21 e_1'). Moreover, many of these allowed bands are predicted to be very weak so that there are only 7 transitions in C_{50} and 9 transitions in C_{70} with a relative intensity of more than 5%. The most intense band always corresponds to a C=C stretching mode (C_{50} 1560 cm^{-1}, C_{60} 1628 cm^{-1}, C_{70} 1592 cm^{-1}). The ratio of the observed[21] and calculated frequency for this band in C_{60} is 0.8778 which is consistent with the fact that the harmonic MNDO frequencies are usually 10–15% higher than the observed fundamental frequencies.[94] Assuming similar errors in C_{50}, C_{60}, and C_{70}, we predict that the most intense infrared band of C_{50} and C_{70} should be observed around 1369 and 1397 cm^{-1}, respectively, with a significant red shift from C_{60} (1429 cm^{-1}).[21] Judging from the calculated spectra a search for these bands should offer the most promising chance for an infrared detection of C_{50} and C_{70}.

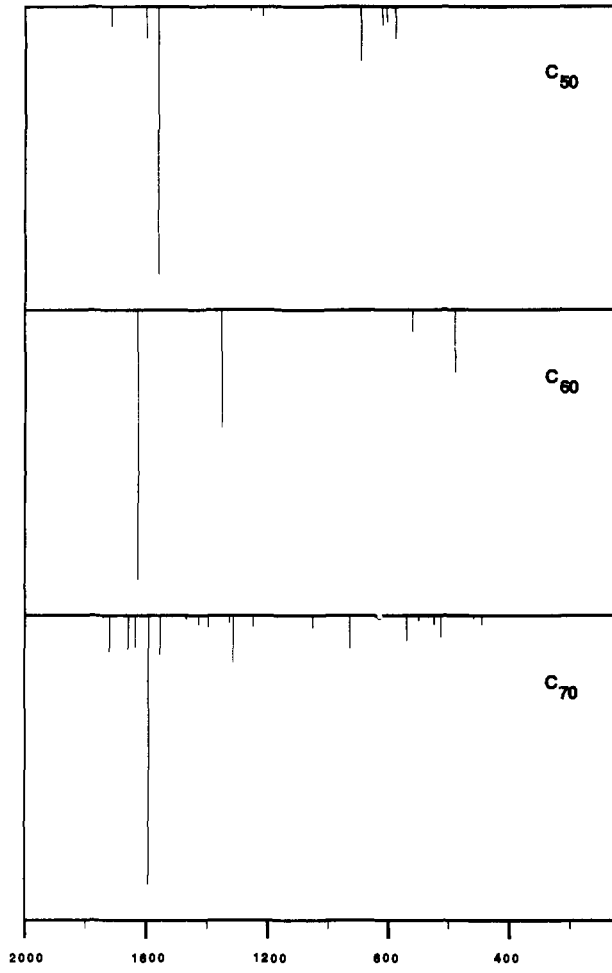

Figure 9. Predicted infrared spectra for the most stable C_{50}, C_{60}, and C_{70} clusters (k = 10, 13, 15).

Figure 10 shows the predicted infrared spectra of C_{120} (k = 26), C_{180}, and C_{240}, with 46 (t_2), 14 (t_{1u}), and 18 (t_{1u}) infrared-allowed transitions, respectively. The strongest bands always occur in the range between 1300 and 1800 cm^{-1}. The calculated spectra for C_{180} and C_{240} are remarkably similar. When used for the experimental identification of these clusters the predicted frequencies should be scaled by a factor of about 0.88 (see above).

E. Cationic Lithium Complexes. Large carbon clusters contain a big cavity and should therefore be able to trap atoms or ions. Experimentally, complexes of various clusters with lanthanum[16,17] and with potassium and cesium cations[12,18] have been found and ascribed to structures with the metal inside the cage[16,18] although a complexation on the outside has also been considered,[12,17] particularly for species with more than one metal atom (e.g. $C_{60}K_3^+$).[12] The ionization potential and electron affinity of $C_{60}La$ have been calculated by a local density approach[102] while the relative energy of $C_{60}Li^+$ has been obtained with MNDO.[52] Both previous theoretical studies assumed an icosahedral structure with the metal at the origin of the cage.

Table V presents some more detailed MNDO results for $C_{60}Li^+$ and $C_{42}Li^+$. Since MNDO is known to exaggerate the interaction between lithium and carbon atoms, the following discussion will focus on qualitative distinctions and trends. The icosahedral structure[52] of $C_{60}Li^+$ with lithium at the origin turns out to be a stationary point with three negative eigenvalues of the force constant matrix. In the minimum for the cage structure lithium

(100) Dewar, M. J. S. *The Molecular Orbital Theory of Organic Chemistry*; McGraw-Hill: New York, 1969; p 176.
(101) Bakowies, D.; Thiel, W. *Chem. Phys.* In press.
(102) Rosén, A.; Wästberg, B. *J. Am. Chem. Soc.* **1988**, *110*, 8701.

Table V. MNDO Results for C_nLi^+ Complexes

system	position of lithium[a]	point group[b]	N_{imag}[c]	ΔH_f,[d] kcal/mol	R,[e] Å	Δx,[f] Å	q_{Li},[g] e
$C_{60} + Li^+$	at infinity	I_h	0	0.0	∞	∞	1.00
$C_{60}^+ + Li$	at infinity[h]	I_h	0	88.2	∞	∞	0.00
$C_{60}Li^+$	at origin	I_h	3	49.7	3.59	−3.36	0.76
	below 5-ring	C_{5v}	2	28.3	2.39	−2.02	0.60
	below 6-ring	C_1	0	27.8	2.41 (4)	−1.92	0.60
	above 5-ring	C_{5v}	0	−53.0	2.29	1.90	0.55
	above 6-ring	C_1	0	−54.5	2.31 (1)	1.82	0.51
	in 5-ring	C_{5v}	1	237.9	1.51	−0.13	−0.05
	in 6-ring	C_1	1	170.6	1.63 (1)	−0.15	0.07
$C_{42} + Li^+$	at infinity	C_s	0	0.0	∞	∞	1.00
$C_{42}^+ + Li$	at infinity[h]	C_s	0	95.7	∞	∞	0.00
$C_{42}Li^+$	below 6-ring	C_1	0	25.5	2.56	−2.08	0.55
	above 5-ring	C_1	0	−59.1	2.24 (6)	1.90	0.49
	above 6-ring	C_1	0	−66.9	2.31 (5)	1.78	0.50
	above 7-ring	C_1	0	−56.1	2.37 (3)	1.68	0.49
	in 6-ring	C_1	1	141.5	1.67 (1)	−0.19	0.08
	in 7-ring	C_1	1	100.2	1.80 (2)	−0.23	0.20

[a] "Below" a ring = inside the cage, "above" = outside. [b] Point group symmetry imposed during the optimization. The actual symmetry may be higher, e.g. at least C_3 for the $C_{60}Li^+$ species labeled C_1. [c] Number of imaginary frequencies. [d] Heat of formation relative to $C_n + Li^+$. Reference values: $C_{60} + Li^+$ 1026.0 kcal/mol, $C_{42} + Li^+$ 1097.9 kcal/mol. [e] Distance of the lithium atom from the carbon atoms in the nearest ring. If these distances vary the average value is given, with the maximum deviation of the last digit in parentheses. [f] Distance of the lithium atom from the center of gravity of the nearest ring, negative for lithium inside the cage. [g] Net charge on lithium. [h] C_n^+ calculated at the optimized geometry of C_n.

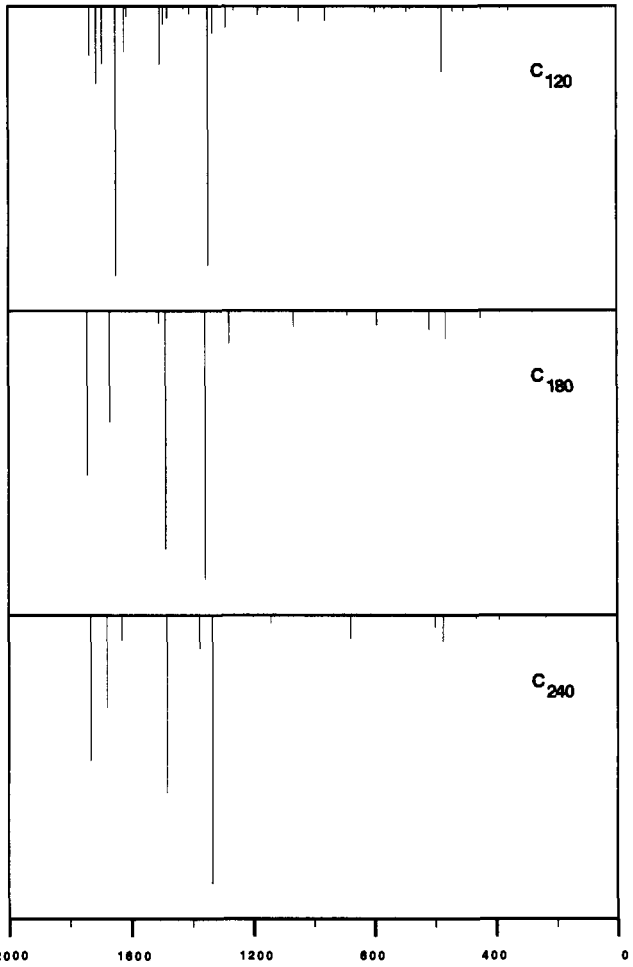

Figure 10. Predicted infrared spectra for the C_{120}, C_{180}, and C_{240} clusters (k = 26, 28, 29).

is located at a distance of about 1.9 Å below a six-membered ring. The barriers between equivalent minima appear to be small so that lithium can be considered to move rather freely on a spherical surface inside the cage at a distance of about 1.4 Å from the origin. The $C_{60}Li^+$ species with lithium inside the cluster are endothermic with respect to $C_{60} + Li^+$. However, there are two complexes with lithium on the outside which are exothermic. The greater stability of the outside complexes may partly be due to simple electrostatics since a charge on the outside can polarize the π electrons of the cluster more effectively than a charge inside and therefore lead to a larger gain in energy.[103] This hypothesis is qualitatively supported by the calculated atomic charges in these complexes. In the transition states for lithium migration through the cage, the lithium atom is located almost in the middle of the five- and six-membered rings, respectively, with a small shift to the inside. The calculated barriers are extremely high so that the complexes with lithium inside the cage should be kinetically inert, once they are formed, regardless of their endothermicity.

Table VI. Computational Performance for MNDO SCF Calculations[a-d]

	C_{60}	C_{120}	C_{180}	C_{240}	C_{540}
N_{AO}	240	480	720	960	2160
SCF cycles	16	24	20	21	24
T_{SCF}, s	4	33	87	204	2404
T_{GRAD}, s	0.4	3.1	3.5	6.3	30.6
MFLOPs/s	188	242	258	270	290
memory, MW	1.2	2.9	5.8	9.8	47.8

[a] Cray Y-MP, sn1511, Unicos (5.1), cft77 (3.1.2), 1 cpu (sn1033 for C_{540}). [b] MNDO90, Version 3.1 of June 7, 1990. [c] SCF accuracy of 10^{-6} ($P_{\mu\mu}$) and 10^{-6} eV (E_{el}). [d] Number of atomic orbitals (N_{AO}), user cpu time for an SCF calculation (T_{SCF}), and an additional gradient evaluation (T_{GRAD}).

The MNDO results for $C_{42}Li^+$ are qualitatively similar to those for $C_{60}Li^+$. The inside minimum again corresponds to a structure where lithium is below a six-membered ring. The most stable of the three outside complexes is the one with lithium above a six-membered ring. The migration of lithium from the inside to the outside requires an activation of about 75 or 126 kcal/mol, for passing through a seven- or six-membered ring, respectively, so that the inside $C_{42}Li^+$ complex is also kinetically inert. A reversible trapping of a lithium cation thus seems to be feasible only for carbon clusters which contain rings of at least eight atoms.

F. Computational Aspects. To our knowledge, this study involves the largest geometry optimizations and force constant calculations which have ever been carried out with MNDO or related quantum-chemical methods. Therefore it seems appropriate to discuss the computational performance of our current semiempirical program[104] in these applications. For this purpose we report benchmark data for five clusters C_n with n = 60, 120, 180, 240, and 540 (k = 13, 26–30) obtained on Cray Y-MP computers.

Table VI summarizes the data for MNDO SCF calculations. It is obvious that the time for a gradient evaluation ($\sim N_{AO}^2$)

(103) Winnewisser, B. Private communication, December 1989.
(104) Thiel, W. Program MNDO90, Version 3.1, July 1990.

Table VII. Computational Performance for MNDO Geometry Optimizations[a-d]

	C_{60}	C_{120}	C_{180}	C_{240}	C_{540}
N_G	2	17	6	7	15
N_{BFGS}	4	33	18	21	23
N_{SCF}	8	63	38	40	35
ΔH_f, kcal/mol					
initial	909	2291	1604	3108	6816
final	869	1202	1392	1596	2580
real time, s					
-1 cpu	15	1169	1643	4376	44144[e]
-8 cpu	3	164	226	588	5733
MFLOPs/s					
-1 cpu	158	216	248	263	290[e]
-8 cpu	796	1543	1784	1949	2201
speedup factor	5.03[f]	7.14	7.20	7.42	7.70[e]

[a] Cray Y-MP/8128, sn1033, Unicos (5.1), cft77 (4.0), dedicated. [b] MNDO90, Version 3.1 of July 30, 1990. [c] SCF accuracy of 10^{-5} ($P_{\mu\mu}$) and 10^{-5} eV (E_{el}). [d] Number of variables (N_G), BFGS cycles (N_{BFGS}), and SCF calculations (N_{SCF}). [e] The MFLOP rate for 1 cpu and the speedup factor were determined in a partial optimization (3 BFGS cycles). The real time for 1 cpu was estimated from this speedup factor and the measured real time for 8 cpus. [f] Possibly not reliable due to overhead in the real time for 8 cpus.

becomes negligible to that for the SCF calculation ($\sim N_{AO}^3$) for the largest clusters (about 1% in the case of C_{540} with N_{AO} = 2160). The most time-consuming steps ($\sim N_{AO}^3$) in the computation represent matrix operations (matrix diagonalization and pseudodiagonalization,[105] formation of the density matrix) and can therefore be vectorized efficiently so that a speed of 290 MFLOPs/s is reached for C_{540} (87% of the hardware limit). Table VII lists the benchmark data for the geometry optimizations which were carried out with a parallelized version of our program. Comparison of the wallclock times for 1 and 8 cpu indicates speedup factors up to 7.7. The complete geometry optimization of C_{540} requires 5733 s of real time and proceeds at a speed of 2201 MFLOPs/s (83% of the hardware limit for 8 cpu). It should be stressed that our program does not exploit symmetry in the time-determining steps ($\sim N_{AO}^3$) of the calculation. Therefore the computational effort for C_{540} (N_{AO} = 2160) should be typical for any closed-shell molecule with a similar number of atomic orbitals, e.g. $C_{360}H_{720}$ (1080 atoms, N_{AO} = 2160). Semiempirical MNDO calculations are therefore quite feasible for molecules with 1000 atoms.

5. Conclusion

The present MNDO study provides many quantitative data on large carbon clusters which allow us to analyze systematic trends and to draw the following qualitative conclusions. (a) Large clusters tend to form planar graphite segments rather than distribute the curvature evenly over the cage. (b) The heat of formation per atom correlates well with the average curvature so that relative stabilities can be estimated from structural data (see eq 4). (c) Curvature-corrected Hückel calculations can reproduce the relative stabilities of clusters without too many five-membered rings, even though the diminished π interaction accounts for typically only 35–40% of the total destabilization energy ΔH_f^{rel} relative to 2D-graphite. Simple force field estimates cover 85 ± 10% of ΔH_f^{rel}. (d) The suggested "magic number" stability[23,24] is reflected in the destabilization energies ΔH_f^{rel} per cluster. However, the thermodynamically relevant stabilities per atom generally increase with increasing cluster size so that C_{540} is considerably more stable than 9 C_{60}. (e) The predicted infrared spectra may facilitate the experimental identification of some stable clusters, especially C_{50} and C_{70}. (f) Cationic lithium complexes with lithium inside the cage are endothemic with respect to $C_n + Li^+$, but kinetically inert, while those with lithium outside the cage are formed exothermically.

6. Addendum

After submission of this paper, the isolation of pure, solid C_{60} and the detection of C_{70} have been reported,[106] with an unambiguous confirmation of the previous[21] experimental infrared data for C_{60}. Vibrational Raman spectra of purified solid films of C_{60} and C_{70} have been published[107] which are compatible with our current theoretical results. Pure samples of C_{60} and C_{70} have been characterized by their mass and ^{13}C NMR spectra.[108] The experimentally deduced C_{70} structure[108] corresponds to the most stable C_{70} isomer considered presently (k = 15). Other ongoing and yet unpublished experimental work on carbon clusters has been summarized.[109]

Note Added in Proof. Several other relevant papers have appeared in the last few weeks.[110-119]

Acknowledgment. This work was supported by the Fonds der Chemischen Industrie and the Alfried-Krupp-Förderpreis. The calculations were carried out on Cray Y-MP computers at HLRZ Jülich and at Mendota Heights, Minnesota. We thank Cray Research for a grant of computer time and Dr. Jan Andzelm and Dr. Brad Elkin for technical help.

Supplementary Material Available: Optimized structures for all carbon clusters C_n ($20 \le n \le 540$), for the planar hydrocarbons C_nH_m ($n = 6k^2$, $m = 6k$, k = 1–6), and for corannulene $C_{20}H_{10}$ including optimized bond lengths and POAV angles (20 pages). Ordering information is given on any current masthead page.

(105) Stewart, J. J. P.; Csaszar, P.; Pulay, P. *J. Comput. Chem.* **1982**, *3*, 227.
(106) Krätschmer, W.; Lamb, L. D.; Fostiropoulos, K.; Huffman, D. R. *Nature* **1990**, *347*, 354.
(107) Bethune, D. S.; Meijer, G.; Tang, W. C.; Rosen, H. J. *Chem. Phys. Lett.* **1990**, *174*, 219.
(108) Taylor, R.; Hare, J. P.; Abdul-Sada, A. K.; Kroto, H. W. *J. Chem. Soc., Chem. Commun.* **1990**, 1423.
(109) Baum, R. M. *Chem. Eng. News* **1990**, *68*(*44*), 22.
(110) Ajie, H.; Alvarez, M. M.; Anz, S. J.; Beck, R. D.; Diederich, F.; Fostiropoulos, K.; Huffman, D. R.; Krätschmer, W.; Rubin, Y.; Schriver, K. E.; Sensharma, D.; Whetten, R. L. *J. Phys. Chem.* **1990**, *94*, 8630.
(111) Haufler, R. E.; Conceiao, J.; Chibante, L. P. F.; Chai, Y.; Byrne, N. E.; Flanagan, S.; Haley, M. M.; O'Brien, S. C.; Pan, C.; Xiao, Z.; Billups, W. E.; Ciufolini, M. A.; Hauge, R. H.; Margrave, J. L.; Wilson, L. J.; Curl, R. F.; Smalley, R. E. *J. Phys. Chem.* **1990**, *94*, 8634.
(112) Johnson, R. D.; Meijer, G.; Bethune, D. S. *J. Am. Chem. Soc.* **1990**, *112*, 8983.
(113) Wilson, R. J.; Meijer, G.; Bethune, D. S.; Johnson, R. D.; Chambliss, D. D.; de Vries, M. S.; Hunziker, H. E.; Wendt, H. R. *Nature* **1990**, *348*, 621.
(114) Wragg, J. L.; Chamberlain, J. E.; White, H. W.; Krätschmer, W.; Huffman, D. R. *Nature* **1990**, *348*, 623.
(115) Meijer, G.; Bethune, D. S. *J. Chem. Phys.* **1990**, *93*, 7800.
(116) Yannoni, C. S.; Johnson, R. D.; Meijer, G.; Bethune, D. S.; Salem, J. R. *J. Phys. Chem.* **1991**, *95*, 9.
(117) Arbogast, J. W.; Darmanyan, A. P.; Foote, C. S.; Rubin, Y.; Diederich, F. N.; Alvarez, M. M.; Anz, S. J.; Whetten, R. L. *J. Phys. Chem.* **1991**, *95*, 11.
(118) Lichtenberger, D. L.; Nebesny, K. W.; Ray, C. D.; Huffman, D. R.; Lamb, L. D. *Chem. Phys. Lett.* **1991**, *176*, 203.
(119) Scuseria, G. E. *Chem. Phys. Lett.* **1991**, *176*, 423.